Heterogeneous nucleation and wetting of water thin films on a metal surface: A study by optical second harmonic generation

Minchul Yang and Hai-Lung Dai

Citation: The Journal of Chemical Physics **118**, 5106 (2003); doi: 10.1063/1.1553793
View online: http://dx.doi.org/10.1063/1.1553793
View Table of Contents: http://scitation.aip.org/content/aip/journal/jcp/118/11?ver=pdfcov
Published by the AIP Publishing

Heterogeneous nucleation and wetting of water thin films on a metal surface: A study by optical second harmonic generation

Minchul Yang[a] and Hai-Lung Dai[b]
Department of Chemistry, University of Pennsylvania, Philadelphia, Pennsylvania 19104-6323

(Received 19 September 2002; accepted 26 December 2002)

The condensation of water thin films on a hydrophobic metal surface, Ag(111), was examined using optical second harmonic generation. Condensation coefficient and the fraction of metal surface area covered with water during film deposition were measured in the temperature range of 145–175 K. It was found that under isothermal condensation conditions, the condensation coefficient decreases abruptly to zero at a temperature several degrees lower than that predicted by zero-order desorption kinetics. This catastrophic failure in water film deposition at these temperatures can be explained by the occurrence of wetting–dewetting transition as a result of three-dimensional cluster formation, i.e., the critical nucleus size becomes too large at these temperatures to allow the formation of the first layer and subsequent growth of water film. Model calculations based on classical nucleation theory which depicts that heterogeneous nucleation is the initial step of water film deposition can be used to quantitatively characterize the critical nucleus size as about 100 and the nucleation rate to be slower than 10^{-3} ML s^{-1} at these temperatures. © *2003 American Institute of Physics.*
[DOI: 10.1063/1.1553793]

I. INTRODUCTION

Water films vapor-deposited on a solid surface, whether in the form of crystalline, glass, or liquid, have been a subject of significant relevance to many fields such as atmospheric science,[1–3] astrophysics,[4–6] and tribology,[7] in addition to being of substantial general interest in physics and chemistry.[8–10] For example, cloud formation in the atmosphere is enhanced by heterogeneous nucleation and condensation of water molecules on solid particles.[11,12] Ice films grown on the surface of a foreign object are an important class of substance on satellites of the outer planets, the surfaces of comets, and interstellar grains.[6,13]

The formation of a water film on a solid surface involves heterogeneous nucleation and condensation processes. The rate-determining step of nucleation is the formation of the ''critical nucleus'' defined by the number of water molecules n^*. When the size of the crystallite is smaller than n^*, its free energy increases with the size. Formation of stable crystallites from monomers on a two-dimensional surface means that a free energy barrier must be surmounted. Once their size is larger than n^*, however, growth of the crystallites is thermodynamically favorable because of the more favorable volume-to-surface ratio. Hence determining the size of the critical nucleus and its formation rate has been a central subject for the understanding of the nucleation process.

The technologically important[14–17] metallic and inorganic semiconducting films have been used as model systems for testing heterogeneous nucleation theories. Studies of these strongly bound systems (atom–atom binding energy ~ a few eV) have shown that nucleation and condensation processes are described mainly by three characteristic energies: the adatom adsorption and diffusion energies, and the adatom–adatom pair binding energy.[14,18–20] In the nucleation model for atoms with strong adatom–adatom binding energy, n^* is close to one. This means that these atoms have the tendency to immediately nucleate toward larger clusters and grow into crystalline structure. Experimental techniques that have been used for monitoring cluster formations of the strongly bound systems include Auger spectroscopy,[21] ion scattering (Rutherford backward scattering),[22] and the more recent microscopic techniques[20] such as STM, AFM, and TEM which have made it possible to visualize cluster formation and its growth processes at atomic level.[23,24]

By contrast, weakly bound systems like molecular films present a different set of challenges both theoretically and experimentally. The weak intermolecular forces in molecular films give rise to much larger values of n^*, as the driving force for nucleation can no longer be described simply by the binding energy between molecules. Experimentally, investigating molecular films using the scanning probe techniques has been a challenging task because the dielectric film is perturbed by relatively strong tip–film interaction compared with the weak intermolecular and molecule–substrate interactions.[25,26] Although noncontact scanning force microscopy has been successful in imaging water droplets on solid surfaces,[25–27] its effectiveness in monitoring nucleation and condensation processes in molecular films has not been demonstrated.

Our interest here is to understand the nucleation and condensation processes responsible for water films deposition on hydrophobic surfaces of metals such as Ag and Au. The binding energy of water molecules with surfaces such as

[a]Present address: Department of Chemistry, University of California, Berkeley, CA 94720.
[b]Author to whom correspondence should be addressed. Currently at the Department of Chemistry, University of Pennsylvania, Philadelphia, PA 19104-6323. Electronic mail: dai@sas.upenn.edu

Ag(111), Ag(110), or Au(111) is lower than the intermolecular binding energy, making it plausible to form three-dimensional clusters. The formation of three-dimensional water clusters on hydrophobic surfaces was initially proposed from observations made in TPD experiments.[9,28,29] In those experiments, water films prepared in thickness ranging from sub-monolayer to multilayers desorb via zero-order kinetics. The deduced desorption energy is very close to the sublimation energy of ice (51.2 kJ/mol), regardless of the thickness. These observations suggest that desorption of water from hydrophobic metal surfaces occurs through first the formation of three-dimensional clusters and then their sublimation.

The size and formation rate of the critical nucleus is strongly dependent on temperature. According to the classical nucleation theory,[30] as temperature increases, the size of the critical nucleus increases while its formation rate decreases. Consequently at higher temperatures, it is more difficult to form stable ice clusters. This indicates that, in the temperature range where diffusion of water molecules is allowed, increasing temperature induces a change from wetting of the surface with monomers/small-clusters to dewetting of the surface due to the need to form larger clusters during the water film deposition.

In this work, we will show that optical second harmonic generation (SHG) can be used for characterizing two important observables during isothermal deposition of water films on the Ag(111) surface: the film growth rate and the surface coverage. The growth rate is obtained by monitoring the interference pattern in the second harmonic (SH) light generated at the metal surface during film deposition.[31,32] This SH light generated at the Ag(111) surface can also be used to deduce the portion of surface covered by adsorbate molecules.[33] Direct measurement of water coverage on the surface is necessary for monitoring the extent of wetting on the surface. The flat Ag(111) is chosen in this study because of its chemical inertness and because its interaction with water molecules is one of the weakest among metals.

Experimental observations, as illustrated below, indicate that an abrupt suppression in the growth rate during isothermal deposition of water films occurs at a temperature a few degrees lower than the one predicted by the zero-order adsorption/desorption model. We will show that this phenomenon is the result of a wetting–dewetting transition caused by three-dimensional cluster formation during isothermal film deposition at these temperatures. The formation of the clusters is facilitated by the increase of the critical nucleus size, which can be deduced from the interpretation of our experimental observations by the classical nucleation theory.[34] The larger critical nucleus size results in a slower cluster formation rate and therefore inhibits the film deposition.

It should be noted that water adsorption on surfaces have been previously studied with several surface analytical techniques under ultra-high vacuum (UHV) conditions.[9] These previous works included high-resolution electron energy loss spectroscopy,[35,36] TPD,[9,28,29] ellipsometry,[37] and linear-optical reflectivity.[38] There, however, has been no report of observation of nucleation in film deposition and the changeover from wetting to dewetting with temperature increase. This work is the first time that heterogeneous nucleation during water film deposition is proposed and a first quantitative attempt in characterizing the nucleation rate and the size of the critical nucleus.

II. MONITORING THIN FILM DEPOSITION BY OPTICAL SECOND HARMONIC GENERATION: THE THEORETICAL MODEL

A. Film growth rate

Optical interference in second harmonic generation at a surface can be used to measure the growth rate and condensation coefficient of a thin film on that surface. The metal surface, such as Ag(111), due to reduced symmetry, is an intrinsic source for SHG, which can be induced by an intense incident fundamental light pulse. The intensity of the SH light, propagating through and exiting the water film, can be detected at the specula angle. Both the SH and fundamental lights experience multiple reflections inside the film, resulting in the interference of these light fields. Consequently, the SH intensity as a function of film thickness exhibits oscillatory patterns as the film grows thicker. The SH intensity, detected from the film-deposited Ag(111), $I^{2\omega}$, can be related to the SH intensity generated from the clean Ag(111) surface, $I^{2\omega}_{\mathrm{Ag}}$, as[31]

$$I^{2\omega} = \text{constant} \cdot |T^{\omega}_{02}|^4 |T^{2\omega}_{20}|^2 I^{2\omega}_{\mathrm{Ag}}. \tag{1}$$

Here T^{ω}_{02} is the transmission factor that describes the transmission of the fundamental light at frequency ω from the vacuum (medium 0), through the film (medium 1), onto silver (medium 2) and $T^{2\omega}_{20}$ is for the SH light at the frequency 2ω transmitting from silver to the vacuum. The transmission factors, T_{02}, can be expressed as $[(t_{01}t_{12}e^{-i\delta})/(1+r_{01}r_{12}e^{-2i\delta})]$, where t and r are transmission and reflection coefficients, respectively, relevant to the interface between media defined by the indices. The phase difference δ is defined as $(2\pi/\lambda)(n-ik)d$, where λ is wavelength, d thickness of the film, and n and k respectively the real and imaginary parts of the refractive index of the film. Assuming a linear film growth rate during film deposition so that the growth rate G is related to the film thickness as $d=Gt$, we have

$$|T_{02}| = \left| \frac{t_{01}t_{12}e^{-(k+in)(2\pi/\lambda)Gt}}{1+r_{01}r_{12}e^{-2(k+in)(2\pi/\lambda)Gt}} \right|. \tag{2}$$

Equation (2) shows that $|T_{02}|$ displays periodicity of $[\lambda/(2Gn)]$ with exposure time. This oscillation in transmission factors for both the fundamental and SH lights results in the observed oscillatory pattern of SH intensity that can be used to deduce the film thickness as a function of exposure and the growth rate.

In the case of loss of light by scattering or absorption within the film, $|T_{02}|$ would show an exponential decrease with a decay constant $k(2\pi/\lambda)G$. If there is no absorption by the water molecules at the fundamental and SH wavelengths, Rayleigh scattering[39] is the primary mechanism for

light intensity decay, we expect theoretically $K_{2\omega}=16K_{\omega}$, where the scattering coefficients K_{ω} and $K_{2\omega}$ are defined as $K=2\pi k/\lambda$.

B. Condensation coefficient

If adsorption/desorption follow zero-order kinetics, the film growth rate G can be expressed as

$$G=\alpha\frac{F_i}{\rho} \tag{3}$$

in which F_i is the incidence flux in unit of number of molecules per unit area and time, α the condensation coefficient, and ρ the density of the film. The incidence flux F_i is given as $F_i=P/(2\pi mRT)^{0.5}$ where P is the partial pressure and M molar mass of water.

The condensation coefficient, α, is defined as $\alpha=(F_a-F_d)/F_i$,[38] where F_a is the adsorption flux and F_d desorption flux. Since desorption of ice films follows zero-order kinetics,[38,40] $F_d=k_0\exp(-E_{des}/kT)$ with desorption energy E_{des}. Finally the condensation coefficient, α, is given as

$$\alpha=S-\frac{k_0\exp(-E_{des}/kT)}{F_i}, \tag{4}$$

where S $(=F_a/F_i)$ is the sticking probability. Assuming S and k_0 are independent of substrate temperature, α decays exponentially with $1/T$.

Experimentally the temperature dependence of α can be obtained by measuring the film growth rate, G, during isothermal deposition of a film. To determine G, SH intensity is measured as a function of exposure time, t. By fitting the SHG experimental result to Eq. (1), we get the value of $4\pi nG/\lambda$, which is set as a variable in the fitting. Assuming the refractive index n and film density ρ are independent of temperature, $4\pi nG/\lambda$ becomes proportional to α at constant F_i according to Eq. (3). The assumption of temperature-independent n and ρ is justified by previous measurements indicating that they vary within a few % in the range of 120–140 K.[38,41] For temperatures between 150 and 170 K, the range of interest in our work, the ice film is believed to be in the same phase. Thus it is unlikely that these two parameters will change more than a few % in this range. For our analysis, this amount of change is negligible.

To deduce α from the measured values of $4\pi nG/\lambda$, it was assumed that $\alpha=1$ at 85 K where water molecules were reported to condense with a sticking probability $S=1$.[38] Therefore α at temperature of T is given as $\alpha(T)=[(4\pi nG/\lambda)\text{ at }T]/[(4\pi nG/\lambda)\text{ at }85\text{ K}]$.

III. EXPERIMENT

All experiments were performed in an ultrahigh vacuum (UHV) chamber with a base pressure of 1×10^{-10} Torr. The Ag(111) surface was cleaned routinely by several cycles of sputtering and annealing before experiment. Water (>99.9%, Aldrich research grade) was purified by several freeze–pump–thaw cycles before use. Water molecules were deposited on the clean Ag(111) surface using a leak valve. The sample temperature was maintained within ±0.1 K during the deposition and optical measurement.

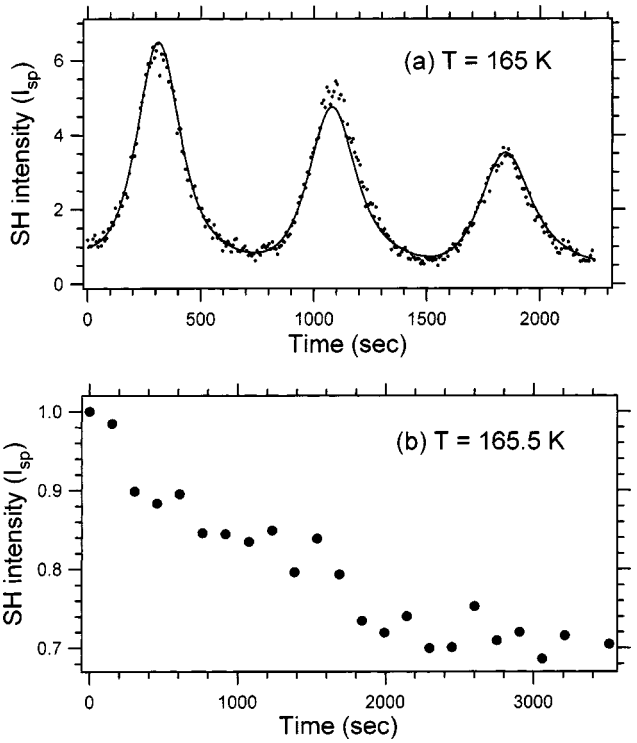

FIG. 1. SH intensity change during an ice film growth. The substrate temperature was kept at (a) 165 K and (b) 165.5 K. The dosing pressure was 2×10^{-6} Torr for both (a) and (b). In (a), the solid line represents the fit of the experimental results (dots) to Eq. (1). The measured SH intensity, I_{sp}, is *s*-polarized fundamental and *p*-polarized SH light.

The 532 nm output from a Nd:YAG laser (Continuum 580 A, 8 ns pulse length, 15 mJ/pulse in 4.5 mm diameter, linearly polarized with 60° incident angle) was used as the fundamental light. The SH light generated at the silver surface, propagating along with the fundamental light and exiting the ice film, was passed through a filter/monochromator assembly and detected by a photomultiplier during film deposition at a fixed temperature. Detailed arrangement of the nonlinear optical experimental setup can be found elsewhere.[32]

IV. RESULTS AND ANALYSIS—TEMPERATURE DEPENDENCE OF CONDENSATION COEFFICIENT

The water film thickness measured by the SHG technique during isothermal deposition can be used to determine the film growth rate, which subsequently allows the condensation coefficient α as a function of surface temperature to be deduced through the use of the relation between G and α in Eq. (3). Figure 1(a) shows the variation of SH intensity during water deposition on the Ag(111) surface at a constant temperature of 165 K. The SH intensity oscillates with exposure time due to optical interference of the fundamental and SH lights within the water film. The height of the peaks decreases as the film becomes thicker due to light scattering from ice crystallites formed in the film at this temperature.

For experiments with the dosing pressure set at 2×10^{-6} Torr, the oscillatory pattern with decreasing peak intensity in SHG output occurs in the temperature range of 145.0 and 165.0 K. At temperatures above 165.5 K, however,

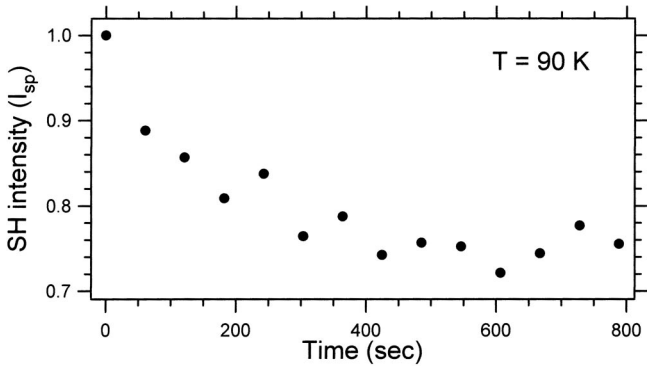

FIG. 2. SH intensity change at 90 K under dosing pressure of 5×10^{-9} Torr.

it was found that the oscillation of the SH intensity disappears drastically and completely, as shown in Fig. 1(b). At temperatures above 165.5 K, the SH intensity decays slowly and monotonically, and flattens out after an exposure about 4000 L (2000 s at dosing pressure of 2×10^{-6} Torr). This SH intensity pattern [in Fig. 1(b)] is very similar to that shown in Fig. 2 where the SH intensity flattens out after deposition of a single monolayer at 90 K with 2 L of exposure (400 s at 5×10^{-9} Torr).

In Fig. 1(a), the slow decrease of the peak heights with increasing film thickness is due to loss of light through Rayleigh scattering within the film. Crystallization of supercooled water occurs in the range of 140–150 K.[4,42,43] Coexistence of supercooled water and crystalline phases persists in the temperature range 140–210 K.[44] The appearance of the oscillatory pattern clearly indicates that the films have grown to thickness of the order of light wavelength. The inhomogeneous films would result in scattering of both the fundamental and SH lights. In fact in our experiments, when a water film was growing in the range of 140–165 K, scattering of the fundamental beam (532 nm) could visually be observed through naked eye. The scattered light became intensified as the film thickness increased. In contrast, no light scattering was visually observed during water deposition at 165.5 K or higher temperatures.

The absence of oscillation in the SH intensity in Fig. 1(b) is not a result of light scattering—there is a lack of visual detection of scattering and there is no other experimental indication of film growth at these higher temperatures. The SH light intensity pattern in Fig. 1(b) can, however, be understood by comparing it to the one in Fig. 2. The slow decrease in the SH intensity in Fig. 2 is caused by formation of a single monolayer of water on the Ag(111) surface resulted from only 2 L exposure at 90 K. The effect of adsorbates on SHG from metal surfaces has been discussed in literature.[33,45] Polarization of electrons at the surface, which is the main contributor to SHG at the metal surface, can be reduced by adsorbate binding to the surface, resulting in a decrease in the SH intensity generated from the metal surface. The variation of the SH intensity has proven to be linearly related to adsorbate coverage on the metal surface.[33,45] Since the saturation coverage of water on Ag(111) is 1.05×10^{15} cm^{-2},[28] it would take 2 L exposure to reach saturation. The time span at 5×10^{-9} Torr dosing pressure for reaching the minimum of the SH intensity in Fig. 2 agrees qualitatively with that predicted for reaching the saturation coverage of the water monolayer on metal.

The slow decrease in SH intensity in Fig. 1(b), where the surface is exposed to much higher water vapor pressure for a long period, can be understood with a similar cause as that in Fig. 2. The much higher exposure of the Ag surface-to-water vapor at 165.5 K does not appear to result in the growth of a water film, evidenced by the lack of SH intensity oscillatory pattern. Instead, the SH intensity behavior at 165.5 K is consistent with the assumption that the saturation coverage of the water monolayer occurs after about 4000 L of exposure. This amount of exposure is 2000 times higher than that required for the saturation coverage of water at 90 K. It is likely that at 165.5 K, desorption rate has increased greatly to make the deposition of the water film implausible. Consequently, we can assign $\alpha=0$ at 165.5 K and higher temperatures where the SH intensity does not display oscillatory behavior.

The value of $4\pi nG/\lambda$ for any given temperature between 145 and 165 K can be determined by fitting the SH intensity oscillatory pattern to Eq. (1). In this temperature range, the film growth rate is determined by a competition between adsorption and evaporation. Using the relation, $\alpha(T)=[(4\pi nG/\lambda)\text{ at }T]/[(4\pi nG/\lambda)\text{ at }85\text{ K}]$, the condensation coefficient α can be deduced for any given temperature. In Fig. 3, the condensation coefficient α (filled circles), determined as a function of the surface temperature at two different dosing pressures 2×10^{-6} and 5×10^{-6} Torr, is plotted. As predicted from Eq. (4), α decays smoothly with T until desorption rate suddenly increases at 165.5 K for dosing pressure of 2×10^{-6} [Fig. 3(a)] and 168.0 K for 5×10^{-6} Torr [Fig. 3(b)]. In Fig. 3(b), α shows a slower decay than in Fig. 3(a) simply because the incidence flux, F_i, in Fig. 3(b) is higher than in Fig. 3(a).

The points (filled circles) in Figs. 3(a) and 3(b) can be fitted to Eq. (4) to yield the desorption energy: 50.6 ± 0.4 kJ/mol and 50.5 ± 0.4 kJ/mol, respectively. These values compare with the sublimation energy of ice, 51.2 kJ/mol.[46] The fitted curves, as predicted by Eq. (4) and shown as solid lines in Figs. 3(a) and 3(b), indicate that α goes to zero at 169 and 173 K, respectively. This model prediction is in dire contrast to experimental measurements of α which shows that in isothermal deposition, zero-deposition occurs at 165.5 and 168 K, respectively. This disagreement in temperature of several degrees between the zero-condensation temperature extrapolated from the desorption model of Eq. (4) and the experimentally observed zero-condensation temperature under isothermal deposition condition is the most remarkable observation in Fig. 3. For reasons that will become apparent in discussions below, we define the extrapolated zero-condensation temperature as the ideal zero-condensation temperature, T_0, and the zero-condensation temperature experimentally measured under isothermal deposition condition the nucleation temperature, T_n.

The ideal zero-condensation temperature T_0, predicted by Eq. (4) which is established according to steady-state

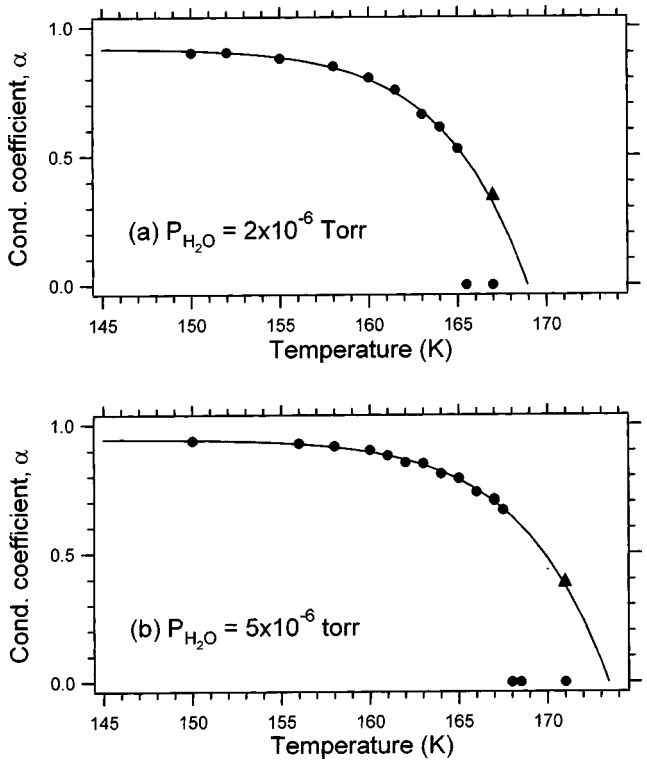

FIG. 3. Condensation coefficient, α, measured as a function of substrate temperature. Dosing pressure used in (a) was 2×10^{-6} and in (b) 5×10^{-6} Torr. The fit (solid line) to Eq. (2) gives for (a) $S=0.92$, $k_0=4.12\times10^{16}$, and 50.6 ± 0.4 kJ/mol, and (b) $S=0.94$, $k_0=1.55\times10^{16}$, and 50.5 ± 0.4 kJ/mol. The filled circles are determined from isothermal deposition experiments. The triangles are the values obtained by measuring the rate of decrease in thickness of a film, prepared at 150 K, whose temperature was then raised to the indicated value. See text for details.

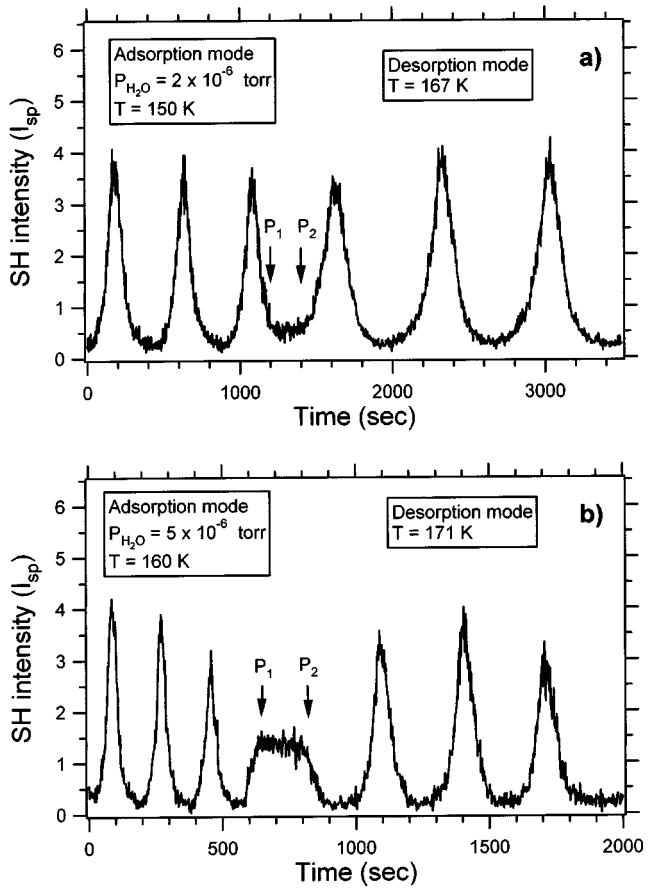

FIG. 4. Variation of SH intensity with time t in adsorption and desorption mode for dosing pressure of (a) 2×10^{-6} and (b) 5×10^{-6} Torr. Ice films were deposited at (a) 150 K and (b) 160 K until $t=P_1$, and then temperature started ramping at $t=P_2$ to reach (a) 167 K and (b) 171 K at 1 K/s. The time period between P_1 and P_2 was necessary for pumping residual water in the chamber.

zero-order evaporation-condensation kinetics over an ice film, can actually be demonstrated experimentally. Take Fig. 3(a) as an illustration. It is important to recognize that if a thick water film can actually be deposited at the temperatures between 165.5 and 169 K, evaporation-condensation equilibrium will be reached over the film surface to allow the condensation coefficient predicted by Eq. (4) to be measured. However, since we know that the deposition of ice films is not allowed in this temperature range under isothermal deposition condition, the ice films have to be first prepared at a temperature lower than 165.5 K and then heated up to a temperature between 165.5 and 169 K. The vaporization rate of this film can then be measured from the thickness change of the film as a function of time by using the SHG technique similarly to that described in Sec. II A.

The ice films with a thickness of about 1 μm were first deposited at 150 and 160 K in two separate experiments under a pressure of 2×10^{-6} and 5×10^{-6} Torr, respectively. The vacuum chamber was then rapidly pumped down to below 5×10^{-9} Torr, and the surface quickly heated (hearing rate$=1$ K/s) up to either 167 [in Fig. 3(a)] or 171 K [in Fig. 3(b)]. At these elevated temperatures, desorption occurs from the surface of the ice film in zero-order kinetics with an increased vaporization rate, resulting in the decrease of film thickness which can be determined from the SH intensity oscillatory pattern. Figure 4 shows the decrease of the film thickness as indicated by the SH intensity interference pattern in this set of experiments. Equation (4) is then used to determine α, shown as filled triangles in Fig. 3, according to the measured desorption flux, F_d. It is clear that the desorption model, as expressed in Eq. (4), does hold at any temperature if the desorption-condensation equilibrium can be established over the surface of a deposited ice film.

While the condensation coefficient, as a function of temperature, of ice films follows faithfully Eq. (4), it is also clear that *under isothermal deposition condition* when deposition is conducted at a temperature higher than the nucleation temperature T_n, the deposition does not commence according to the rate predicted by Eq. (4). This contradiction can be understood as such that under isothermal deposition condition at temperatures higher than the nucleation temperature T_n, water molecules do not wet on the surface for film growth, instead they nucleate into clusters and sublimate from the beginning so that multilayer films cannot be grown.

V. DISCUSSION-DEPOSITION OF WATER FILMS ON METAL AS DESCRIBED BY THE CLASSICAL NUCLEATION THEORY

The experimental observations made on the condensation coefficient, α, of water molecules on Ag(111) in the

temperature range between 150 and 171 K can be summarized as the following. As long as deposition can generate wetted layers on the metal surface and desorption-condensation occurs over the surface of the film, the condensation coefficients can be described by the model depicted by Eq. (4), over the entirety of this temperature range. It appears that, however, under isothermal deposition condition, film deposition and growth can be achieved only for the lower temperature portion of this range. Under isothermal deposition condition, water films fail to deposit on the metal surface and α prematurely reaches zero at temperatures nearly 3 degrees below the ideal zero-condensation temperature T_0 predicted by Eq. (4). The most logical interpretation of this observation is that water film growth is suppressed abruptly at temperatures higher than T_n because of the wetting/dewetting transition of water on Ag(111). At $T>T_n$ water molecules do not wet on the surface but nucleate to form clusters from which sublimation occurs.

The realization of zero-condensation at temperatures lower than T_0 in isothermal deposition is resulted from the difference between sublimation rates of three-dimensional ice clusters and wetted ice films. The underlying assumption of the condensation model of Eq. (4) is that adsorption/desorption event occurs from the surface of the flat ice film, which can be described by zero-order adsorption/desorption kinetics. In zero-order kinetics, the film growth and sublimation rates are independent of the film thickness. Initial stage of the ice film formation, however, is a heterogeneous process. If water–surface bonding is strong in comparison with intermolecular interaction, water molecules will form a two-dimensional monolayer on the surface. This is the case of complete wetting. The single monolayer can then serve as a template for continuing film growth and the temperature dependence of α can be predicted by Eq. (4).

Now we explain the abrupt suppression of α at T_n under isothermal deposition condition using the classical nucleation theory. The critical nucleus size n^* and the nucleation rate are crucial for determining if the initial stage in film growth—the formation of a monolayer of ice clusters as a template for further film growth—can be accomplished within the experimental time. Strong hydrogen bonding between water molecules tends to lead to the formation of three-dimensional ice clusters, which occurs even at 155 K as suggested from TPD results.[9,46]

In classical nucleation theory, n^* is a strong function of *supersaturation*, $\Delta\mu(T)$, as $n^*\propto(\Delta\mu)^{-3}=[(E_{\rm sub})(T_n-T)/T_n]^{-3}$.[47] In addition to n^*, another criteria in determining whether wetting or dewetting occurs is the rate of critical nuclei formation per unit area, J_s. For quantitative discussion, we also need to define *saturation time*, t_s, which is the time span for critical nuclei to cover the whole area of metal surface, and given as

$$t_s=[A_b J_s]^{-1}, \tag{5}$$

where A_b is basal area of a critical nucleus. The saturation time, t_s, is a parameter to determine if wetting or dewetting occurs. Importantly, it is directly related to the surface area adsorbed with water and can be measured by the SHG experiments as shown in Figs. 1(b) and 2.

All these parameters n^*, J_s, and t_s can be calculated using the classical nucleation theory[34] with boundary conditions deduced from our experimental results. The calculations will show that J_s and t_s decrease dramatically around T_n and that film growth is negligible on the timescale of our experiments at temperatures higher than T_n.

According to the classical nucleation theory,[34] heterogeneous nucleation begins with adsorption of monomers on a foreign surface. The monomer concentration of water molecules on surface $n_1=F_i\times\tau_a$, where F_i is the incidence flux and τ_a the average residence time of an adsorbed water. The average residence time $\tau_a=\tau_0\exp(E_{ads}/kT)$ where E_{ads} is the adsorption energy. Note that E_{ads} is different from the sublimation energy, $E_{\rm sub}$, for ice. Monomers diffuse on the substrate to form ice clusters, whose formation is related to density fluctuation of monomers on the surface. Clusters smaller than n^* are quickly evaporated. We assume that the critical nucleus is cap-shaped, characterized by the contact angle θ.[34]

There are three main stages in first-order phase transition from monomers to clusters: nucleation, coalescence and aging.[34] Our concern here is only the nucleation stage. We adapt ''stationary nucleation condition'' in which the cluster size distribution is time-independent. Under this condition, an n-sized cluster increases its size mostly by monomer attachment with attachment frequency f_n, rather than through coalescence of smaller clusters. This is justified since at the nucleation stage, number density of monomers, n_1, is dominant over that of clusters.[34] For diffusion-controlled nucleation process, the attachment frequency can be calculated as $f_n=\gamma_n c^* D_s\tau_a$, where γ_n is the sticking coefficient, D_s the surface-diffusion rate, and c^* ($\sim$1 to 5) the so-called capture number due to surface diffusion.[34] The surface-diffusion rate is given as $D_s=D_0\exp(-E_{\rm diff}/kT)$, where $E_{\rm diff}$ is diffusion activation energy of water molecules on Ag(111). The size of a cluster decreases via monomer detachment process. The detached monomer desorbs eventually.

The stationary nucleation rate, $J_s(T)$, is given as zf^*C^*,[34] where f^* is attachment frequency for critical nuclei of size n^*. The equilibrium concentration of critical nuclei, C^*, is given as $C^*=C_0\exp(-W^*/kT)$ where C_0 is the concentration of nucleation sites. The free energy barrier is determined as $W^*=(16\pi/3)[\Psi(\theta)v_0^2\sigma^3/\Delta\mu^2]$, where σ is the surface energy of the vacuum/ice interface. The molar volume, v_0, is the reciprocal of ice density. The shape factor, $\Psi(\theta)$, is given as $\Psi(\theta)=0.25(2+\cos\theta)(1-\cos\theta)^2$ for a cap-shaped entity. The numerical factor z, the *Zeldovich* factor, is given as $z=n^*(W^*/3\pi kT)^{1/2}$. Finally, the stationary nucleation rate, J_s, is given by[34]

$$J_s=\frac{(T_0-T)^2}{8\pi v_0 E_{\rm sub}^2 T_0^2}\left(\frac{1}{kT\psi(\theta)\sigma^3}\right)^{1/2} f^* C_0 \times\exp\left(-\frac{\psi(\theta)16\pi v_0^2\sigma^3 E_{\rm sub}^2 T_0^2}{3kT(T_0-T)^2}\right), \tag{6}$$

$$f^*=\gamma_n c^*\tau_0 D_0\frac{P}{\sqrt{2\pi MRT_\nu}}\exp\left(\frac{E_{ads}-E_{\rm diff}}{kT}\right), \tag{6a}$$

where T_ν is the temperature of water vapor.

TABLE I. Parameters used for calculations of the nucleation process as shown in Fig. 5.

Name of constants	Values	Remarks
Zero-sublimation temperature, T_0	169.0 K	[a]
Nucleation temperature, T_n	165.5 K	[a]
Sublimation energy, E_{sub}	50.6 kJ/mol	[a]
Adsorption energy, E_{ads}	40.0 kJ/mol	[b]
Surface diffusion energy, E_{dif}	8 kJ/mol	[b]
Surface free energy, σ	77 mJ/m^2	[c]
Volume per molecule, υ_0	3.22×10^{-29} m^3	[d]
Pre-exponential factor, τ_0	10^{-13} s	[e]
Pre-exponential factor, D_0	10^{-4} cm^2/s	[e]
Dosing pressure, P	2×10^{-6} Torr	[a]
Contact angle, θ	37°	[f]
Sticking coefficient, γ_n	1	[g]
Capture number, c^*	1	[g]
Density of nucleation sites, C_0	1.38×10^{15} cm^{-2}	[h]

[a]This experiment.
[b]Based on the value 40.7 kJ/mol (Ref. 48) or 42.3 kJ/mol (Ref. 49) measured for water/Pt. The adsorption energy for water on silver is expected to be lower than for water/Pt. Surface diffusion energy is estimated as 20% of the adsorption energy (Ref. 9).
[c]Set as the same as the ice surface free energy at 248 K (Ref. 50). The surface energy of a cluster increases as temperature decreases or as the size of the cluster increases. For a nonometer-sized cluster of our interest at 165.5 K its surface energy may have similar magnitude to that of ice at 248 K as the two effects with opposite trends should balance each other out.
[d]Volume per molecule in ice bulk at 160 K (Ref. 38).
[e]Estimated.
[f]Estimated based on the values: 30° for water/graphite (Ref. 51) and 40° for water/Pt (Ref. 52). See text.
[g]Estimated.
[h]Surface density of silver atoms on Ag(111).

We present calculations for the case with dosing pressure $P=2\times10^{-6}$ Torr [Fig. 3(a)] as an example. The stationary nucleation rate, $J_s(T)$, and size of critical nucleus, n^*, are calculated based on the set of physical quantities listed in Table I[48–52] and plotted as a function of the surface temperature, T, in Fig. 5.

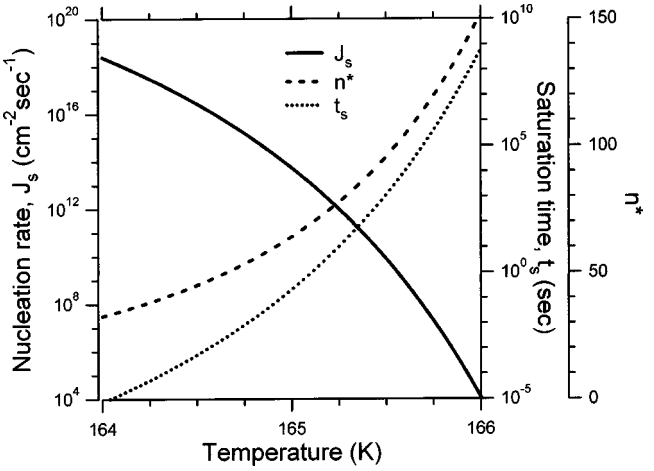

FIG. 5. Critical nucleus formation rate $J_s(T)$ (solid line), saturation time t_s (dotted line), and critical nucleus size n^* (dashed line) calculated as a function of substrate temperature by using the classical nucleation theory. The parameters used for calculations shown in this graph are listed in Table I. The calculation is based on the boundary condition that at 165.5 K, $t_s=2000$ s.

Although many parameters appear in Eq. (6), only the few parameters in the exponent actually induce the most significant changes in $J_s(T)$. Especially, θ is the most crucial factor in determining $J_s(T)$. It was found that variation of even 1 degree of θ changed one order of magnitude for $J_s(T)$. We set up one constraint to minimize the uncertainty of θ. As seen in Fig. 1(b), it takes a few thousand seconds of dosing time for the silver surface to be fully covered by water molecules. This indicates that the saturation time t_s is a few thousand seconds. This experimental result is used as a boundary condition for determining $J_s(T)$, n^*, and θ:θ is first manually adjusted to affect $J_s(T)$ such that the calculated t_s is placed at a few thousand seconds. We find that the best results were produced when the contact angle is set at 37°. Other pre-exponential factors such as γ_n, c^*, τ_0, and D_0 were simply estimated because of the lack of experimental determination. Their uncertainties, however, could change $J_s(T)$ no larger than a couple of orders of magnitude. More importantly, they are independent of surface temperature. Consequently their uncertainties do not affect the rate of change of the parameters shown in Fig. 5.

It is clear from Fig. 5 that $J_s(T)$ and t_s vary almost 14 orders of magnitude when the surface temperature is lowered by only 2 degrees from 166 to 164 K. These abrupt changes in $J_s(T)$ and t_s correspond directly to the observation of the abrupt depression in α at 165.5 K. A careful examination of the behavior of the three parameters in Fig. 5 explains in terms of the nucleation process the dramatic change in isothermal condensation of water on Ag. We will focus the discussion on the three temperatures 166, 165.5, and 165 K in Fig. 5.

It is essential that at any given temperature and dosing pressure, a first layer of water molecules, whether as monomers or as critical size clusters, can be formed on the metal surface as the basis to support film growth within the experimental timescale. For the three temperatures of interest we consider the formation of a layer of critical size nuclei. The probability of this occurring can be estimated as follows. First we recognize that approximately 10^{15} water molecules per cm^2 are needed to cover the metal surface. The probability of the surface area being covered by the critical size clusters of size n^*, with approximately $(n^*)^{2/3}$ number of molecules at the base of a single cluster, would be roughly $[J_s\times(n^*)^{2/3}\times(\text{experimental timescale})/10^{15}]$. At 165.5 K, J_s is $\sim10^{10}$ cm^{-2} s^{-2} and $n^*\sim100$. If we set the experimental timescale as 2000 s, the probability of the formation of a layer of critical size clusters is just about unity. Of course these conditions are primarily determined by our setting t_s at around the experimental timescale for this temperature. At 165 K, n^* has decreased to about 60 while J_s increased by four orders of magnitude to shorten t_s to less than 1 s. Water films can in this case grow on the basis of this rapidly formed layer of saturated stable clusters. Correspondingly, at 166 K, the time for the formation of saturated layer of stable clusters ($n^*\sim150$) has reached 10^9 s! Within the experimental timescale, no film growth at this temperature is plausible.

To summarize the discussion, a mechanistic model for deposition of water films on metal surfaces that is consistent

with the classical nucleation theory begins to emerge. The model is for the temperature range where diffusion of water molecules on the metal surface is allowed. At the low temperature side of this temperature range, the critical nucleus size of water clusters is small, approximately between 1 and 10. The time (or exposure) for the formation of a first layer of molecules to support further film growth is much faster than 1 s (or requiring ~1 L exposure). Here, the structure of the first layer has not been determined but it should consist of monomers or stable small clusters. As temperature increases, ice sublimation rate increases and the critical nucleus size also increases. Nucleation of somewhat larger, three-dimensional clusters dominates on the metal surface as water molecules condense. At a few degrees below the ideal zero-condensation temperature, n^* approaches 100 and the time required for the build up of the first layer of such clusters now begin to exceed experimental timescale and deposition of water films does not occur.

VI. CONCLUDING REMARKS

In this work, the nonlinear optical SHG technique allows us to simultaneously monitor the condensation coefficient α, through real-time measurement of film growth rate, and the fraction of metal surface covered with water molecules. The latter can be used to directly assess the wetting of water films on the surface. These experimental capacities are crucial for the characterization of isothermal condensation of water films on metal and provided the critical information for the deduction of the water film deposition mechanism.

The most significant observation is the abrupt suppression of α, under isothermal condensation condition, at temperatures several degrees lower than those predicted by zero-order kinetics of desorption over multiplayer water films. This is the result of a wetting–dewetting transition on the metal surface caused by dramatic changes in the heterogeneous nucleation of water molecules on the metal surface.

It is interesting to see that the classical heterogeneous nucleation theory, developed mainly based on observations of atomic systems, can be applied to this molecular system in a detailed and quantitative manner to account for the observations. The formation rate and size of the critical nucleus in heterogeneous nucleation can be calculated using observable such as zero-condensation temperature, sublimation energy, and surface coverage. The classical nucleation theory depicts that for the thin film to grow, a layer of stable, critical size clusters as foundation for further growth has to be deposited on surface first. The wetting to dewetting transition can be predicted and understood as a failure to form within the experimental time (10^3 s) this first layer of the critical size ($n^*=100$) water clusters on the Ag surface at the temperatures of concern.

This work demonstrates a new experimental method for studying the deposition of molecular films as well as illustrates the importance of heterogeneous nucleation in the formation and growth of systems with weak intermolecular interactions.

ACKNOWLEDGMENTS

This work is supported by a grant from the Air Force Office of Scientific Research. The equipment needed for this work was acquired and supported by NSF MRSEC program, Grants No. DMR96-32598 and No. DMR00-79909.

[1] S. Solomon, R. R. Garcia, F. S. Rowland, and D. J. Wuebbles, Nature (London) **321**, 755 (1986).
[2] R. Zellner, *Global Aspects of Atmospheric Chemistry* (Springer, New York, 1999).
[3] M. A. Zondlo, S. B. Barone, and M. A. Tolbert, J. Phys. Chem. A **102**, 5735 (1998).
[4] P. Jenniskens and D. F. Blake, Astrophys. J. **473**, 1104 (1996).
[5] E. Mayer and R. Pletzer, Nature (London) **319**, 298 (1986).
[6] A. Kouchi, Nature (London) **330**, 550 (1987).
[7] *Handbook of Micro/nano Tribology*, edited by B. Bhushan (CRC, Boca Raton, 1999).
[8] P. V. Hobbs, *Ice Physics* (Clarendon, Oxford, 1974).
[9] P. A. Thiel and T. E. Madey, Surf. Sci. Rep. **7**, 211 (1987).
[10] *Water: A Comprehensive Treatise*, edited by F. Franks (Plenum, New York, 1972).
[11] J. B. Mason, *The Physics of Clouds* (Oxford University Press, London, 1971).
[12] H. R. Pruppacher and J. D. Klett, *Microphysics of Clouds and Precipitation* (Reidel, Boston, 1978).
[13] *Ices in the Solar System*, edited by J. Klinger, D. Benest, A. Dollfus, and R. Smoluchowski (Reidel, Dordrecht, 1985).
[14] *Growth and Properties of Ultrathin Epitaxial Layers*, edited by D. A. King and D. P. Woodruff (Elsevier, New York, 1997).
[15] C. Argile and G. E. Rhead, Surf. Sci. Rep. **10**, 277 (1989).
[16] T. Michely, M. Hohage, M. Bott, and G. Comsa, Phys. Rev. Lett. **70**, 3943 (1993).
[17] W. D. Luedtke and U. Landman, Phys. Rev. B **40**, 11733 (1989).
[18] J. A. Venables, Phys. Rev. B **36**, 4153 (1987).
[19] J. A. Venables, G. D. T. Spiller, and M. Hanbucken, Rep. Prog. Phys. **47**, 399 (1984).
[20] M. Zinke-Allmang, L. C. Feldman, and H. Grabow, Surf. Sci. Rep. **16**, 377 (1992).
[21] M. Zinke-Allmang, L. C. Feldman, and S. Nakahara, Appl. Phys. Lett. **51**, 975 (1987).
[22] M. Zinke-Allmang, L. C. Feldman, S. Nakahara, and B. A. Davidson, Phys. Rev. B **39**, 7848 (1989).
[23] S. Hope, M. Tselepi, E. Gu, T. M. Parker, and J. A. C. Bland, J. Appl. Phys. **85**, 6094 (1999).
[24] Y. Wakayama, T. Inokma, and S. Hasegawa, J. Cryst. Growth **183**, 124 (1998).
[25] A. Gil, J. Colchero, M. Luna, J. Gomez-Herrero, and A. M. Baro, Langmuir **16**, 5086 (2000).
[26] J. Hu, X.-D. Xiao, D. F. Ogletree, and M. Salmeron, Science **268**, 267 (1995).
[27] L. Xu, A. Lio, J. Hu, D. F. Ogletree, and M. Salmeron, J. Phys. Chem. B **102**, 540 (1998).
[28] M. Klaua and T. E. Madey, Surf. Sci. **136**, L42 (1984).
[29] B. D. Kay, K. R. Lykke, J. R. Creighton, and S. J. Ward, J. Chem. Phys. **91**, 5120 (1989).
[30] A. Laaksonen, V. Talanquer, and D. W. Oxtoby, Annu. Rev. Phys. Chem. **46**, 489 (1995).
[31] C. M. Li, Z. C. Ying, and H. L. Dai, J. Chem. Phys. **101**, 7058 (1994).
[32] T. Sjodin, T. Troxler, and H. L. Dai, Langmuir **16**, 2832 (2000).
[33] M. Asscher and Z. Rosenzweig, in *Laser Spectroscopy and Photochemistry on Metal Surfaces*, Vol. 1, edited by H. L. Dai and W. Ho (World Scientific, Singapore, 1995), pp. 90.
[34] D. Kashchiev, *Nucleation; Basic Theory with Application* (Oxford, Boston, 2000).
[35] H. Ibach and S. Lehwald, Surf. Sci. **91**, 187 (1980).
[36] D. V. Chakarov, L. Osterlund, and B. Kasemo, Langmuir **11**, 1201 (1995).
[37] D. Beaglehole and H. K. Christenson, J. Phys. Chem. **96**, 3395 (1992).
[38] D. E. Brown, S. M. George, C. Huang, E. K. L. Wong, K. B. Rider, R. S. Smith, and B. D. Kay, J. Phys. Chem. **100**, 4988 (1996).
[39] I. P. Hermann, *Optical Diagnostics for Thin Film Processing* (Academic, San Diego, 1996).

[40] R. J. Speedy, P. G. Debenedetti, R. S. Smith, C. Huang, and B. D. Kay, J. Chem. Phys. **105**, 240 (1996).
[41] M. S. Westley, G. A. Baratta, and R. A. Baragiola, J. Chem. Phys. **108**, 3321 (1998).
[42] W. Hage, A. Hallbrucker, E. Mayer, and G. P. Johari, J. Chem. Phys. **100**, 2743 (1994).
[43] P. Jenniskens and D. F. Blake, Science **265**, 753 (1994).
[44] P. Jenniskens, S. F. Banham, D. F. Blake, and M. R. S. McCoustra, J. Chem. Phys. **107**, 1232 (1997).
[45] S. G. Grubb, A. M. DeSantolo, and R. B. Hall, J. Phys. Chem. **92**, 1419 (1988).
[46] I. Kohl, E. Mayer, and A. Hallbrucker, Phys. Chem. Chem. Phys. **2**, 1579 (2000).
[47] D. Kashchiev, J. Chem. Phys. **76**, 5098 (1982).
[48] K. Raghavan, K. Foster, K. Motakabbir, and M. Berkowitz, J. Chem. Phys. **94**, 2110 (1991).
[49] B. A. Sexton and A. E. Hughes, Surf. Sci. **140**, 227 (1984).
[50] L. Makkonen, J. Phys. Chem. **101**, 6196 (1997).
[51] M. Luna, J. Colchero, and A. M. Baro, J. Phys. Chem. B **103**, 9576 (1999).
[52] A. C. Zettlemeyer, J. Colloid Interface Sci. **28**, 343 (1968).